

## Supporting Information

# Oxidation of Amino Acids by Peracetic Acid: Reaction Kinetics, Pathways and Theoretical Calculations

Penghui Du<sup>a,b,d</sup>, Wen Liu<sup>b,c</sup>, Hongbin Cao<sup>a</sup>, He Zhao<sup>a</sup>, Ching-Hua Huang<sup>b\*</sup>

<sup>a</sup> *Beijing Engineering Research Center of Process Pollution Control, Division of Environment Technology and Engineering, Institute of Process Engineering, Chinese Academy of Sciences, Beijing 100190, China*

<sup>b</sup> *School of Civil and Environmental Engineering, Georgia Institute of Technology, Atlanta, Georgia 30332, United States*

<sup>c</sup> *The Key Laboratory of Water and Sediment Sciences, Ministry of Education, College of Environmental Science and Engineering, Peking University, Beijing 100871, China*

<sup>d</sup> *University of Chinese Academy of Sciences, Beijing 100049, China*

\* Corresponding author.

Tel: +1 4048947694; Email address: ching-hua.huang@ce.gatech.edu (C.-H. Huang).

### **Text S1. Quantification of amino acids**

Amino acids were derivatized following previous methods (Newton et al., 1981; Donzanti and Yamamoto, 1988) with modifications before analysis. CYS was derivatized with mBBr and subsequently analyzed by HPLC coupled to a fluorescence (FLR) detector. Stock solution of the mBBr (10 mM) was prepared in acetonitrile; this solution was stable for up to six months at -20 °C. The stock solution was diluted to 100 µM with borate buffer (0.1 M, pH 8.8) before using for the derivatization of CYS. The derivatization was performed in a HPLC vial insert with 150 µL CYS sample and 150 µL borate buffer containing the 100 µM mBBr. The mixture was vortexed for 30 seconds before analysis. FLR detection was operated at an excitation wavelength of 395 nm and an emission wavelength of 475 nm.

The other amino acids were derivatized with OPA, a fresh solution of 70 mg OPA, 1 mL methanol, and 95 mL of buffer (pH 10.5, 25 g/L boric acid, 0.2% 2-mercaptoethanol) was prepared, which was stable up to 1 week at 4 °C. The derivatization was performed in a HPLC vial with 100 µL amino acids sample and 200 µL OPA working solution. The mixture was agitated for 1 min before analysis. FLR detection was operated at an excitation wavelength of 340 nm and an emission wavelength of 455 nm.

## Text S2. Condensed Fukui function method

Fukui function, an important concept in conceptual density functional theory, has been widely used in prediction of reactive sites of electrophilic, nucleophilic, and radical attacks (Parr and Yang, 1984). Fukui function is defined as:

$$f(r) = \left[ \frac{\partial \rho(r)}{\partial N} \right]_v \quad (1)$$

where  $\rho(r)$  is the electron density at a point  $r$  in space,  $N$  is total electron number in present system, and the constant term  $v$  in the partial derivative is external potential. In the condensed version of Fukui function, atomic population number is used to represent the amount of electron density distribution around an atom. The condensed Fukui function can be calculated as follows:

$$\text{Electrophilic attack: } f^-(r) = \rho_N(r) - \rho_{N-1}(r) \quad (2)$$

$$\text{Nucleophilic attack: } f^+(r) = \rho_{N+1}(r) - \rho_N(r) \quad (3)$$

$$\text{Radical attack: } f^0(r) = [f^+(r) + f^-(r)]/2 = [\rho_{N+1}(r) - \rho_{N-1}(r)]/2 \quad (4)$$

where  $q^k$  is the atom charge of atom  $k$  at corresponding state. The reactive sites usually have larger values of Fukui index than other regions. We calculated the condensed Fukui index ( $f^-$ ) of amino acid molecules for electrophilic attacks, as PAA is a strong electrophile reagent which is more likely to attack sites that can readily lose electrons (De Vleeschouwer et al., 2007; Zhang et al., 2017). In this study, Natural Population Analysis (NPA) charge was used as it is considered to be one of the most suitable methods to calculate Fukui index (Olah et al., 2002). A color gradient for the set of Fukui values was generated using the conditional formatting tool in Microsoft Excel 2013.

### Text S3. Local Nucleophilicity Index calculations

The local nucleophilicity index ( $N_k$ ) is calculated based on the global nucleophilicity index ( $N$ ), which was proposed as the inverse of electrophilicity index ( $1/\omega$ ) (Chattaraj and Maiti, 2001). The global electrophilicity index  $\omega$  was defined as follows (Parr et al. 1999):

$$\omega = \frac{\mu^2}{2\eta} \quad (5)$$

where  $\mu$  is the electronic chemical potential (Parr et al., 1978) and  $\eta$  is the chemical hardness (Parr and Pearson, 1983). For an  $N$ -electron system with external potential  $v(r)$  and total energy  $E$ , the electronic chemical potential  $\mu$ , the negative of electronegativity  $\chi$ , is defined as the partial derivative of the energy of the number of electrons at constant external potential and in the absence of a magnetic field:

$$\mu = -\chi = \left( \frac{\partial E}{\partial N} \right)_{v(r)} \approx -\frac{I + A}{2} \quad (6)$$

where  $I$  and  $A$  are the vertical ionization potential and electron affinity, respectively. These two quantities were calculated, again using the B3LYP method and 6-31G(d,p) as basis set. Meanwhile, the chemical hardness  $\eta$  was defined as differentiating the chemical potential to the number of electrons, again at constant external potential:

$$\eta = \left( \frac{\partial^2 E}{\partial N^2} \right)_{v(r)} \approx I - A \quad (7)$$

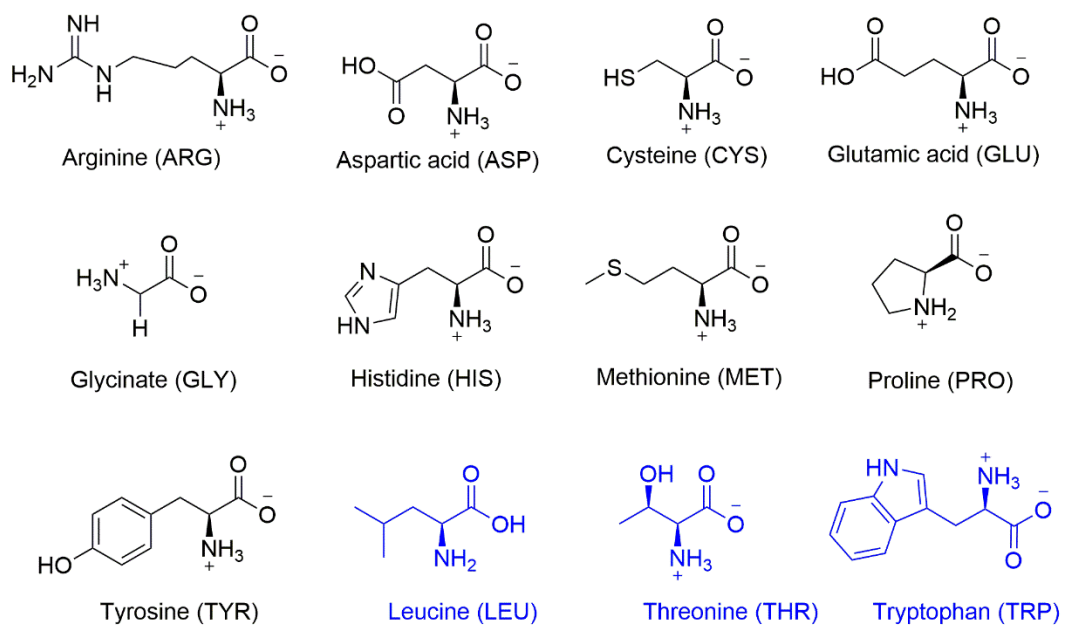


Figure S1. Structures of amino acids used in this work (Amino acids in blue were only used in theoretical prediction purpose).

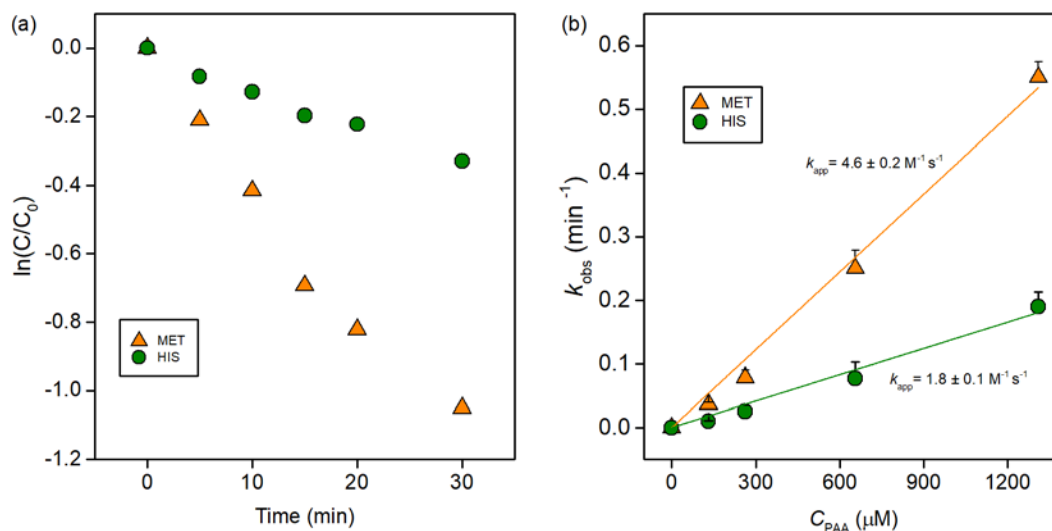


Figure S2. Degradation kinetics of MET and HIS by PAA solution. (a)  $\ln(C/C_0)$  versus time,  $[PAA]_0 = 131 \mu\text{M}$ , (b) Relationship between the initial PAA concentration and pseudo-first-order rate constants for degradation of MET (orange triangles) and HIS (green circles). Solid lines represent linear regressions of second-order reaction kinetics with the fitting parameter  $k_{app}$ . Experimental conditions:  $[\text{amino acids}]_0 = 10 \mu\text{M}$ ,  $[PAA]_0 = 131\text{-}1310 \mu\text{M}$ ,  $\text{pH} = 7.0$ , room temperature).

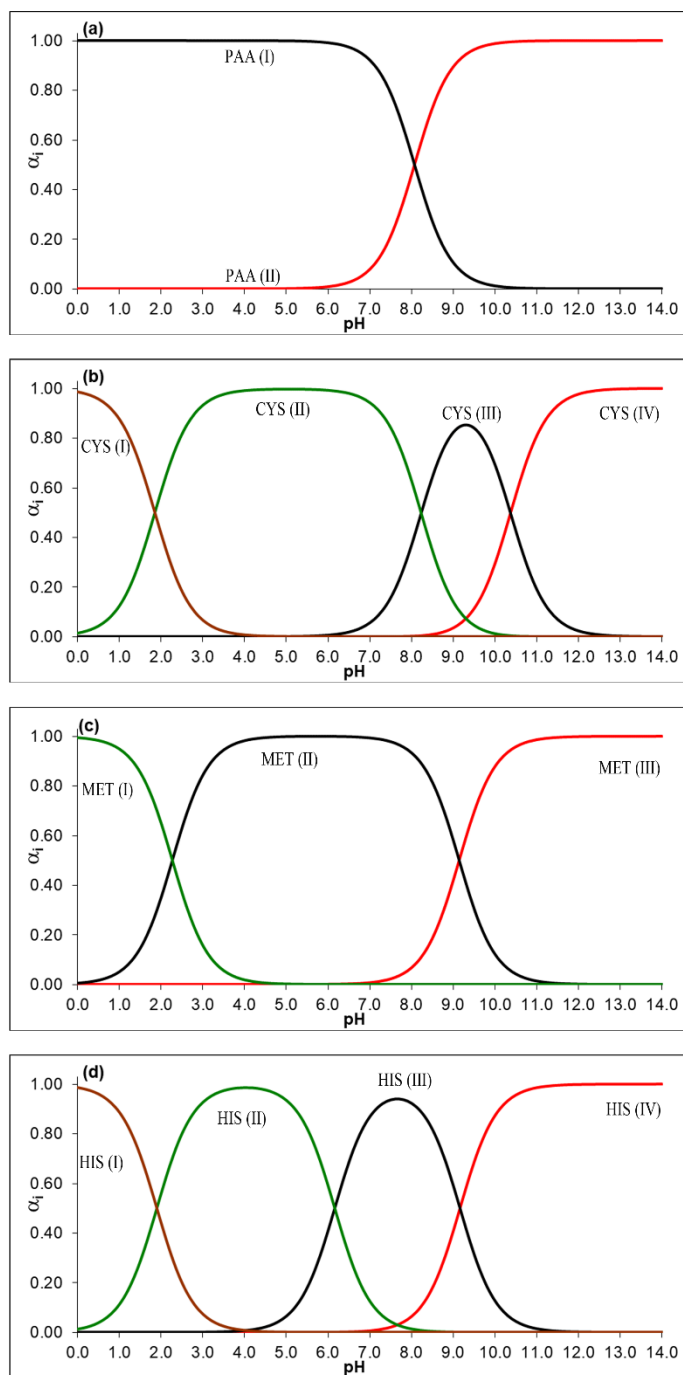


Figure S3. Acid-base speciation of PAA (a), CYS (b), MET (c), and HIS (d).  $\alpha$  is the fraction of the PAA species.

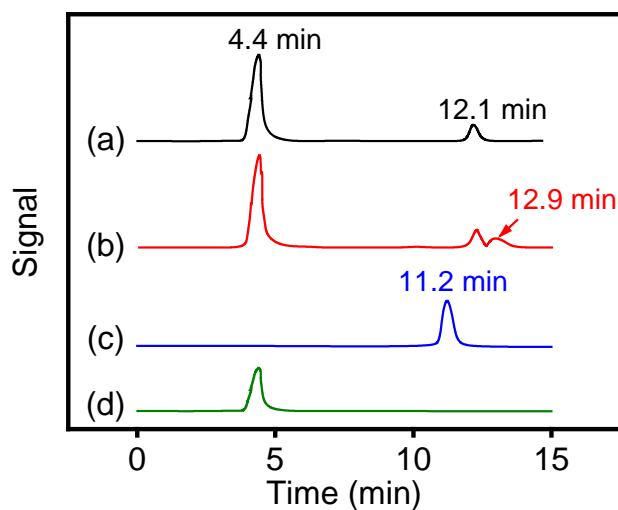


Figure S4. Ion chromatography of (a) 131  $\mu\text{M}$  PAA solution, (b) 131  $\mu\text{M}$  PAA+ 10  $\mu\text{M}$  CYS solution (incubation 30 min), (c) 1  $\mu\text{M}$   $\text{SO}_4^{2-}$  solution, and (d) 1  $\mu\text{M}$  acetic acid.

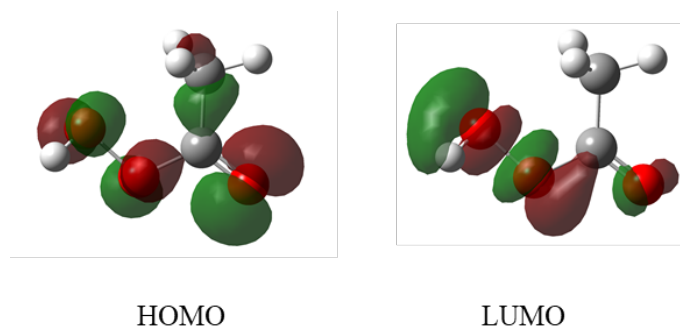


Figure S5. Molecular orbitals of PAA structure. (HOMO: Highest occupied molecular orbital; LUMO: Lowest unoccupied molecular orbital.)



Table S1. Species distribution (in fractions) of PAA and selected amino acids at pH 5, 7, and 9.

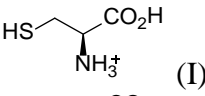
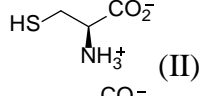
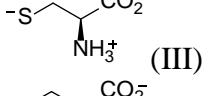
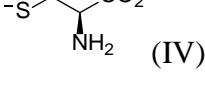
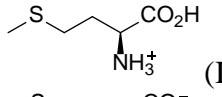
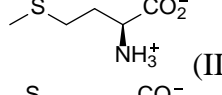
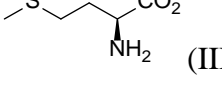
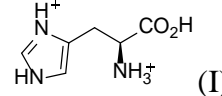
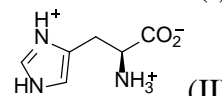
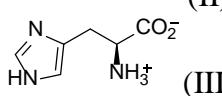
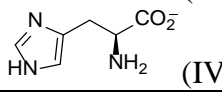
	Species	pH 5	pH 7	pH 9
PAA	$\text{CH}_3\text{C}(=\text{O})\text{OOH}$ (I)	0.999	0.921	0.104
	$\text{CH}_3\text{C}(=\text{O})\text{OO}^-$ (II)	0.001	0.079	0.896
CYS	 (I)	0.001	0.000	0.000
	 (II)	0.998	0.944	0.139
	 (III)	0.000	0.056	0.826
	 (IV)	0.000	0.000	0.035
MET	 (I)	0.002	0.000	0.000
	 (II)	0.998	0.993	0.577
	 (III)	0.000	0.007	0.423
HIS	 (I)	0.001	0.000	0.000
	 (II)	0.934	0.124	0.001
	 (III)	0.065	0.870	0.588
	 (IV)	0.000	0.006	0.411

Table S2. Cartesian coordinate of ARG

Symbol	X	Y	Z
C	0.96854	0.68678	0.65422
C	2.18616	0.59161	-0.28343
N	3.23174	1.61061	-0.05742
C	2.86520	-0.79940	-0.24470
O	4.18714	-0.74964	-0.46047
O	2.26886	-1.83671	-0.06531
H	1.25583	0.31529	1.64762
H	1.84393	0.71872	-1.31964
H	4.39634	0.21444	-0.50545
H	2.98205	2.49430	-0.49123
H	0.72756	1.75214	0.77451
C	-0.27530	-0.05966	0.15582
H	-0.03288	-1.11279	0.00017
H	-0.58473	0.34950	-0.81425
C	-1.44996	0.05279	1.13716
H	-1.19131	-0.45149	2.07381
H	-1.63256	1.10927	1.39489
N	-2.66211	-0.57303	0.62687
H	-3.14555	-1.18479	1.26949
C	-3.50900	0.09299	-0.25528
N	-4.65707	-0.65679	-0.53639
H	-5.19728	-0.20920	-1.26644
H	-4.46656	-1.62884	-0.75103
N	-3.35594	1.24842	-0.79433
H	-2.55521	1.73956	-0.39920
H	3.34221	1.78954	0.93904

Table S3. Cartesian coordinate of ASP

Symbol	X	Y	Z
C	0.58472	0.97371	-0.49207
C	-0.71662	0.64179	0.25639
N	-1.84673	1.54386	-0.01496
C	-1.16386	-0.80913	-0.02247
O	-2.49152	-0.98109	0.03144
O	-0.38433	-1.70738	-0.23754
H	0.46148	0.85494	-1.57159
H	-0.51803	0.68369	1.33329
H	-2.86101	-0.07570	0.15215
H	-1.77657	2.40269	0.52196
H	0.83868	2.02373	-0.29780
C	1.79302	0.14843	-0.08953
O	2.64865	-0.24535	-0.84477
O	1.85603	-0.02403	1.25491
H	2.64649	-0.56499	1.41949
H	-1.87815	1.80258	-0.99899

Table S4. Cartesian coordinate of CYS

Symbol	X	Y	Z
C	0.76698	-0.58185	-0.42422
C	-0.23422	0.16341	0.47401
N	-0.14833	1.61597	0.28297
C	-1.64858	-0.32320	0.07824
O	-2.34424	0.57527	-0.63002
O	-2.05438	-1.42774	0.35299
H	0.59787	-0.31328	-1.47171
H	0.61018	-1.65615	-0.32271
H	-0.07366	-0.15355	1.51269
H	-1.75486	1.36785	-0.67337
H	-0.41540	2.10728	1.13183
S	2.53415	-0.16392	-0.11989
H	2.60032	-0.65768	1.13422
H	0.81141	1.88604	0.07456

Table S5. Cartesian coordinate of GLU

Symbol	X	Y	Z
C	1.16814	0.33917	-0.43143
N	1.46178	1.71492	0.00957
C	2.34164	-0.58213	-0.01432
O	3.45421	0.08531	0.31823
O	2.26464	-1.78826	-0.02187
H	1.18713	0.34254	-1.52973
H	3.20083	1.03758	0.26001
H	1.08622	2.41041	-0.62636
C	-0.17025	-0.24491	0.04105
H	-0.18621	-1.30453	-0.22763
H	-0.21794	-0.19790	1.13555
C	-1.38330	0.48276	-0.56173
H	-1.34251	1.54924	-0.30454
H	-1.39238	0.39756	-1.65142
C	-2.70781	-0.05536	-0.06500
O	-2.80865	0.03349	1.28635
H	-3.67606	-0.34019	1.51718

Table S6. Cartesian coordinate of GLY

Symbol	X	Y	Z
C	0.64106	-0.79643	0.10179
C	-0.69377	-0.03693	0.00422
O	-1.75955	-0.59783	-0.08210
O	-0.55236	1.29573	0.05320
H	0.60912	-1.62604	-0.61275
H	0.67677	-1.24063	1.10180
N	1.77586	0.12148	-0.07178
H	0.42283	1.44135	0.10566
H	2.55503	-0.11912	0.53132
H	2.11676	0.11101	-1.02838

Table S7. Cartesian coordinate of HIS

Symbol	X	Y	Z
C	-3.08107	0.82213	-0.00063
N	-1.80624	0.95313	0.29771
C	-1.27664	-0.32701	0.27297
C	-2.26126	-1.23036	-0.04620
N	-3.40971	-0.48286	-0.21647
C	0.17233	-0.57334	0.56419
C	1.13255	0.10750	-0.43810
N	1.04927	1.57562	-0.34530
C	2.57252	-0.34016	-0.10404
O	3.31906	0.63439	0.42942
O	2.96349	-1.47241	-0.27817
H	-3.80316	1.62356	-0.07006
H	-2.24973	-2.30297	-0.16063
H	-4.32445	-0.83947	-0.44652
H	0.41343	-0.20408	1.56974
H	0.38569	-1.64502	0.55252
H	0.90733	-0.27390	-1.44226
H	2.70974	1.41888	0.43394
H	0.11892	1.85433	-0.03013
H	1.19802	1.99907	-1.25730

Table S8. Cartesian coordinate of MET

Symbol	X	Y	Z
C	-0.04311	-0.36915	-0.14744
C	-1.29313	0.37390	0.34698
N	-1.50613	1.72302	-0.21079
C	-2.56775	-0.47256	0.10506
O	-3.64361	0.26047	-0.21161
O	-2.59281	-1.67467	0.22620
H	-0.07075	-0.42071	-1.24421
H	-0.09883	-1.39944	0.21353
H	-1.23173	0.48475	1.43830
H	-3.30663	1.18697	-0.26500
H	-1.01160	2.43469	0.31684
C	1.25848	0.29110	0.31064
H	1.30091	1.33699	-0.01684
H	1.32598	0.27735	1.40521
S	2.70212	-0.60040	-0.38897
C	4.05224	0.40821	0.31319
H	4.98920	-0.02841	-0.03876
H	3.99635	1.44441	-0.03174
H	4.04106	0.38111	1.40617
H	-1.17399	1.77205	-1.17187

Table S9. Cartesian coordinate of PRO

Symbol	X	Y	Z
C	-1.46654	-0.01682	0.00186
O	-1.57654	-1.20116	-0.61125
O	-2.31907	0.84096	-0.02576
C	-0.13073	0.16533	0.75828
C	0.68202	1.35078	0.19313
H	-0.39068	0.32372	1.81017
C	1.99425	-0.63390	-0.08086
C	1.63481	0.66992	-0.80216
H	1.25418	1.82682	0.99683
H	0.03093	2.10522	-0.25202
H	2.78510	-0.45049	0.66101
H	2.34554	-1.41853	-0.75827
H	2.51556	1.27148	-1.04058
H	1.11339	0.45027	-1.74071
N	0.72259	-1.03708	0.56732
H	0.88111	-1.53403	1.43708
H	-0.71114	-1.64513	-0.41007

Table S10. Cartesian coordinate of TYR

Symbol	X	Y	Z
C	0.92879	-0.24847	0.80814
C	1.81868	-0.09980	-0.45030
N	1.65469	1.22974	-1.06017
C	3.28968	-0.28554	-0.02657
O	3.98921	0.85844	0.00461
O	3.74744	-1.35978	0.28660
H	1.20718	0.53605	1.52187
H	1.18787	-1.20677	1.26822
H	1.58099	-0.92075	-1.13838
H	3.35159	1.54380	-0.31276
H	1.80370	1.18681	-2.06488
C	-0.55229	-0.17406	0.50965
C	-1.29855	0.97265	0.80456
C	-1.22109	-1.25157	-0.09532
C	-2.66083	1.05253	0.50607
H	-0.81527	1.81616	1.29195
C	-2.57567	-1.18923	-0.39787
H	-0.67041	-2.16034	-0.32575
C	-3.30352	-0.03016	-0.09836
H	-3.22070	1.95258	0.75111
H	-3.09016	-2.02596	-0.85845
O	-4.63135	-0.02379	-0.41697
H	-5.01935	0.81946	-0.14855
H	0.70812	1.57373	-0.91709

Table S11. Cartesian coordinate of TRP

Symbol	X	Y	Z
C	-1.19630	0.31776	-0.86452
C	-1.96743	-0.18716	0.38297
N	-2.08077	0.87918	1.39034
C	-3.37732	-0.61743	-0.06408
O	-4.34003	0.24849	0.28709
O	-3.58116	-1.62041	-0.70814
H	-1.74638	1.16695	-1.28802
H	-1.23025	-0.48483	-1.60825
H	-1.46373	-1.08420	0.76265
H	-2.10088	0.48852	2.32869
H	-1.26619	1.48819	1.34182
C	0.21711	0.72438	-0.57122
C	1.32759	-0.14410	-0.25286
C	0.70947	2.00773	-0.53520
C	2.46229	0.68483	-0.03759
N	2.05374	1.99162	-0.21436
H	0.20396	2.94157	-0.74020
H	2.64762	2.80233	-0.15752
C	3.83116	-1.21760	0.39311
C	2.72132	-2.06045	0.17902
C	1.47518	-1.53834	-0.14205
C	3.71914	0.16343	0.28683
H	4.79278	-1.65584	0.64261
H	2.84720	-3.13541	0.26513
H	0.62994	-2.19922	-0.31214
H	4.57597	0.81144	0.44771
H	-3.86448	0.94197	0.80758

Table S12. Cartesian coordinate of LEU

Symbol	X	Y	Z
C	0.50611	0.89877	-0.14291
C	-0.80308	0.49432	0.56962
N	-1.77062	1.60621	0.47373
C	-1.42553	-0.74782	-0.09882
O	-2.42927	-0.45946	-0.94005
O	-1.02395	-1.87333	0.09403
H	0.24546	1.22798	-1.15796
H	-0.58044	0.21562	1.60578
H	-2.56368	0.51420	-0.83483
H	-2.38866	1.62682	1.28050
H	0.89945	1.78262	0.38207
C	1.62071	-0.16253	-0.22515
H	1.23136	-1.01751	-0.78973
H	-1.29692	2.50396	0.43186
C	2.81820	0.41488	-0.99456
H	3.25940	1.26652	-0.46167
H	3.60213	-0.33922	-1.11765
H	2.52812	0.76048	-1.99300
C	2.04833	-0.67761	1.15652
H	2.35449	0.14690	1.81347
H	1.24004	-1.23126	1.64066
H	2.90096	-1.35834	1.06435

Table S13. Cartesian coordinate of THR

Symbol	X	Y	Z
C	1.11996	-0.15468	-0.35000
C	-0.06111	0.36830	0.49793
N	-0.22060	1.81479	0.27340
C	-1.36522	-0.34301	0.07168
O	-2.15229	0.42198	-0.69456
O	-1.63286	-1.48367	0.37486
H	0.84182	-0.04712	-1.41142
H	0.13206	0.10848	1.54636
H	-1.68260	1.29505	-0.72612
H	-0.58055	2.26765	1.10910
H	0.69365	2.21724	0.07904
C	1.47872	-1.60633	-0.05199
H	0.62007	-2.26331	-0.20185
H	2.29164	-1.93693	-0.70851
H	1.81415	-1.70302	0.98504
O	2.21300	0.72427	-0.05241
H	2.95706	0.47208	-0.61429



## References

- Chattaraj, P., Maiti, B., 2001. Reactivity dynamics in atom– field interactions: A quantum fluid density functional study. *J. Phys. Chem. A* 105 (1), 169-183.
- De Vleeschouwer, F., Van Speybroeck, V., Waroquier, M., Geerlings, P., De Proft, F., 2007. Electrophilicity and nucleophilicity index for radicals. *Org. Lett.* 9 (14), 2721-2724.
- Donzanti, B.A., Yamamoto, B.K., 1988. An improved and rapid HPLC-EC method for the isocratic separation of amino acid neurotransmitters from brain tissue and microdialysis perfusates. *Life Sci.* 43 (11), 913-922.
- Newton, G.L., Dorian, R., Fahey, R.C., 1981. Analysis of biological thiols: Derivatization with monobromobimane and separation by reverse-phase high-performance liquid chromatography. *Anal. Biochem.* 114 (2), 383-387.
- Olah, J., Van Alsenoy, C., Sannigrahi, A.B., 2002. Condensed Fukui functions derived from stockholder charges: Assessment of their performance as local reactivity descriptors. *J. Phys. Chem. A* 106 (15), 3885-3890.
- Parr, R.G., Donnelly, R.A., Levy, M., Palke, W.E., 1978. Electronegativity: The density functional viewpoint. *J. Chem. Phys.* 68 (8), 3801-3807.
- Parr, R.G., Pearson, R.G., 1983. Absolute hardness: Companion parameter to absolute electronegativity. *J. Am. Chem. Soc.* 105 (26), 7512-7516.
- Parr, R.G., Szentpály, L.V., Liu, S., 1999. Electrophilicity index. *J. Am. Chem. Soc.* 121 (9), 1922-1924.
- Parr, R.G., Yang, W.T., 1984. Density functional-approach to the frontier-electron theory of chemical-reactivity. *J. Am. Chem. Soc.* 106 (14), 4049-4050.
- Zhang, K., Zhou, X., Du, P., Zhang, T., Cai, M., Sun, P., Huang, C.-H., 2017. Oxidation of  $\beta$ -lactam antibiotics by peracetic acid: Reaction kinetics, product and pathway evaluation. *Water Res.* 123, 153-161.